

IMPULSE DETECTORS FOR NOISED SEQUENCES

Rastislav LUKÁČ

Dept. of Electronics and Multimedial Communications
Technical University of Košice
Park Komenského 13, 041 20 Košice
Slovak Republic

Abstract

This paper is focused on a problem of impulse detection in the dynamic image environments corrupted by impulse noise. Using a proposed architecture that includes an impulse detector and the median filter, the effective methods can be designed. Thus, the image points are classified into two classes such as a class of noise free samples and a class of noised image points. In the case of impulse detection the estimate is performed by a median filter whereas a noise free sample is passed on the output without the change i.e. system works as an identity filter.

Keywords

impulse detector, median filter, dynamic noised image sequences, motion compensation

1. Introduction

In noise filtering, a problem is often how to preserve some desired signal features while the noise elements are removed. An optimal situation would arise if the filter could be designed so that the desired features are invariant to the filtering operation and only noise would be affected. Probably, the simple median [8,17] is still most used a nonlinear filter for its properties such as robustness and the noise suppression. Since the median filter is a nonlinear filter and the superposition does not apply, the optimal situation can never be fully obtained.

However, by a proposed connection of an impulse detector [1,16] and the median filter, it is possible to obtain system that realises an optimal filtering, i.e. noise free samples are passed on the output without the change (system works as an identity filter) whereas corrupted elements are estimated by the median filter. The impulse detectors classify the samples into these two classes.

Many algorithms of the impulse detection were developed for gray-scale static images. Thus, the various principles; that are represented by e.g. mean-based E detector [12] and its extensions such as biased Ep detector [12,13] and E detector with a fuzzy decision [16], family of order-statistic detectors [16] (OSD, COSD), local contrast of the

probability (LCP) [3], entropy-based H-detector [6], use of standard deviation is characterised by SDV detector [13] [15], on the desired properties of LUM smoothers based excellent LUMsm detector [7] and neural detector (ND) [14] that utilise the training capability of neural networks; were successfully used in the connection with standard 3x3 median filter. However, the performance of the detector-filter system depends on the accuracy of the impulse detection. This dependence is not the same for all filters, i.e. the use of more accurate impulse detector might improve the performance of one filter considerably more than the performance of another filter. The relationship between the accuracy of the impulse detection and performance of filter cannot be determined analytically, but instead needs to be determined experimentally. On that account the performance of the lonely impulse detectors is evaluated through a number of true and false classified samples. The use of standard objective criteria, e.g. mean absolute error (MAE) or mean square error (MSE) is possible in the case of connection with some filter. More frequently, the proposed architecture consists of the impulse detector and a 3x3 median filter, since, the median is considered as a basic nonlinear filter. Thus, MAE and MSE show the improvements introduced by the use of impulse detector in comparison with the solitary 3x3 median.

This paper is oriented to the performance of some impulse detectors for multidimensional signals such as dynamic image sequences, i.e. spatiotemporal data [5], that is a time sequence of two-dimensional (2D) images. On that account, to analyse detectors performance four operation structures for image sequences were used. However, the 3x3 median filter was still considered.

2. The input set

In the static image area, the performance of impulse detectors (for most frequently used windows) was presented in [3,6,7,12,13] and extended in [16]. In case of these experiments, two-dimensional windows were applied on the two-dimensional signal. However, the image sequence filtering gives more possibilities since an image sequence is 3-dimensional (3-D) dynamic signal. Therefore in this paper, the four detector windows (Fig. 1) are used to capture signal features in the temporal direction, the spatial position and the spatiotemporal position.

In the case of temporal direction, the input set includes samples along the time axis. This way is similar to one-dimensional case, where the temporal correlation between the frames makes itself felt. Thus, the input set W that is determined by the temporal window through three frames (denotes as TW3) (Fig. 1a) can be expressed as

$$W = \{x(n+m, i, j), -1 \leq m \leq 1\} \quad (1)$$

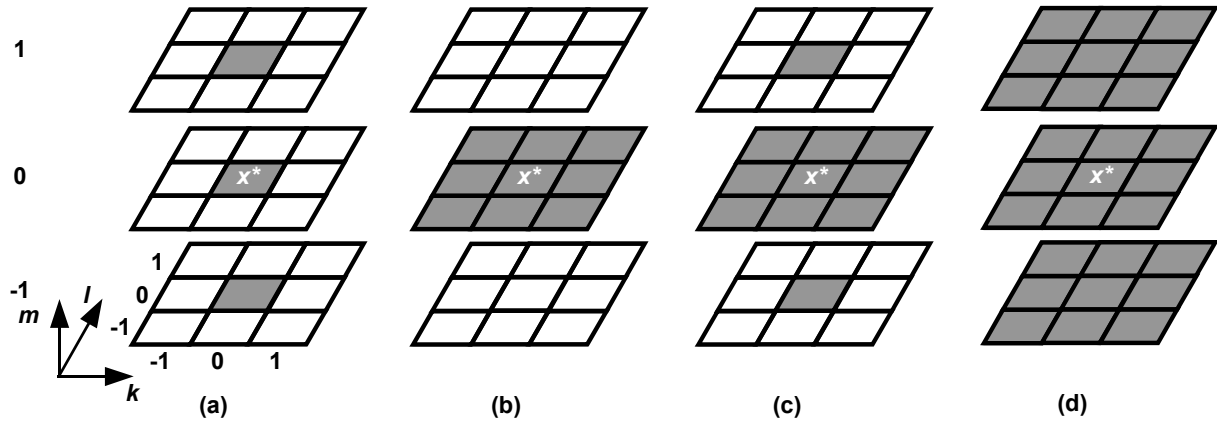


Fig. 1 Operation windows for dynamic image sequences: (a) temporal window – TW3 (b) 3x3 spatial window – 3x3 SW (c) spatiotemporal window - STW_{1,9,1} (d) spatiotemporal cube window – STW_{9,9,9}

Note, that all windows considered in this paper are centred around the central sample x^* . In the sense of subscripting used in this paper, central sample x^* is given by

$$x^* = x(n, i, j) \quad (2)$$

where n denotes time position or a frame item and i, j are indices of sample position in horizontal and vertical directions, separately.

The second window (Fig. 1b) represents the widely used filter window in image filtering. Concerning image sequence processing, in this case the input set includes samples from the processed (actual) frame only, and no information about neighbouring frames is needed. This spatial 3x3 window is denoted as 3x3 SW and the corresponding input set is determined by

$$W = \{x(n, i+k, j+l), -1 \leq (k, l) \leq 1\} \quad (3)$$

Fig. 1c-d shows two spatiotemporal structures that operate in the three frames. Thus, the temporal correlation between the frames and the spatial correlation of the samples within the considered frames are utilised, simultaneously. The first (Fig. 1c) spatiotemporal window (STW_{1,9,1}) is the unification of equations (1) and (3), that is following:

$$W = \{x(n-1, i, j), x(n, i+k, j+l), x(n+1, i, j), -1 \leq (k, l) \leq 1\} \quad (4)$$

The second is the cube window (STW_{1,9,1}) of 27 image points from three frames:

$$W = \{x(n+m, i+k, j+l), -1 \leq (m, k, l) \leq 1\} \quad (5)$$

Note, that all previous input set can be expressed as subsets of the cube window.

For simplification in the following, the reduced description of input samples is used, where the temporal and location indices are replaced by one subscript.

3. Impulse detectors

From the character of impulse noise [10] is known that only some samples are corrupted. Therefore, it can be

desired that impulses are removed only and original image points are invariant to the filtering operation. There is frequent that especially median filtering of noise free pixels bring error into filtration process. On that account were introduced impulse detectors (Fig. 2) that classify samples into a class of noise free pixels and a class of corrupted elements.

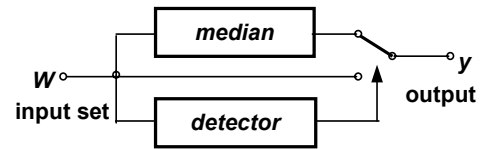


Fig. 2 Proposed architecture of impulse detector and median filter

Thus, this decision is performed on the base of neighbourhood information. In the case of impulse detection the output is equal to the median of input set. On the other hand, no corrupted samples are passed on the output without the change, i.e. system works as an identity filter.

3.1 E detector

The name of E detector [12,13] follows since it is based on the mean value μ of input set. The decision rule of E detector is given by

$$\text{IF } D = M \quad \text{THEN } \textit{median filter} \\ \text{ELSE } \textit{identity filter} \quad (6)$$

where

$$D = |x^* - \mu| \quad (7)$$

$$M = \max_{i=1}^N (|x_i - \mu|). \quad (8)$$

and N is the window size, x_i represents a simplified notation of samples from the input set W .

If the absolute difference D associated with central sample is equal to the maximal absolute difference M then the central sample x^* is probably distorted and therefore should be filtrated.

3.2 SDV detector

To improve the detection property of E detector some its modification (biased Ep detector [13] and E detector control by fuzzy logic [16]) were developed, however the performance (Ep) or complexity (fuzzy E detector) exclude their use in dynamic image sequences. Additional improvement of the E detector was obtained by including standard deviation σ .

$$\sigma = \sqrt{\frac{1}{N} \sum_{i=1}^N (x_i - \mu)^2} \quad (9)$$

to the detector rule and it was called as SDV detector [1]:

$$\begin{aligned} \text{IF } D \geq \sigma \quad \text{THEN } & \textit{median filter} \\ \text{ELSE } & \textit{identity filter} \end{aligned} \quad (10)$$

Thus, if the D (7) is greater than the standard deviation σ (9), the central sample is probably distorted because it is more different from others input samples.

3.3 COSD detector

The central order-statistic detector (COSD) [16] belongs to the class of detectors based on order-statistics. Thus, the input set W must be sorted and the detector rule is given by:

$$\begin{aligned} \text{IF } |\mu - x^*| \geq Tol \quad \text{THEN } & \textit{median filter} \\ \text{ELSE } & \textit{identity filter} \end{aligned} \quad (11)$$

where Tol is the threshold (robust value was found 40) and μ_n is mean of n mid-positioned ordered samples

$$\mu_n = \frac{1}{n} \sum_{i=(n+1)/2}^{N-(n+1)/2} x_{(i)} \quad (12)$$

Thus, the extreme order-statistics (usually outliers) are excluded and the μ_n is determined from probably no corrupted samples.

3.4 LCP detector

Idea of LCP detector [3,6] is based on following rule:

$$\begin{aligned} \text{IF } P^* \geq P_C \quad \text{THEN } & \textit{median filter} \\ \text{ELSE } & \textit{identity filter} \end{aligned} \quad (13)$$

where P_C is a critical value defined as $P_C = 1/N$ and P^* is the local contrast probability (LCP) of processed pixel (i.e. for $i = (N+1)/2$) given by

$$P_i = \frac{C_i}{\sum_{i=1}^N C_i} = \frac{C_i}{C_S}, \quad (14)$$

where N is window size, C_i is associated contrast for any samples from the input set and C^* ($C^* = C_i$ for $i = (N+1)/2$)

is associated contrast of central sample x^* . The associated contrast is defined according to the Weber-Fechner law by

$$C_i = \frac{|x_i - D|}{D}, \quad (15)$$

where D (7) is mean of input set W . Thus, a central pixel is considered as noise and the output value is determined by the median if the local contrast probability of the central sample is greater than or equal to P_C .

3.5 H detector

Unlike LCP detector, on the entropy based H detector [6] utilises the adaptive critical threshold value defined by the following equation:

$$\eta = \frac{-P^* \log P^*}{H} = \frac{-P^* \log P^*}{-\sum_{i=1}^N P_i \log P_i}. \quad (16)$$

Local contrast entropy H is computed in every location of detector window by

$$H = -\sum_{i=1}^N P_i \log P_i \quad (17)$$

where P_i is local contrast probability (14) associated with input sample x_i . The control rule of H detector is determined by the following formula:

$$\begin{aligned} \text{IF } P^* \geq \eta \quad \text{THEN } & \textit{median filter} \\ \text{ELSE } & \textit{identity filter} \end{aligned} \quad (18)$$

3.6 LUMsm detector

The name of LUMsm [7] detector follows from LUM smoothers [2,9], since the outputs for all smoothing levels are used as a base for detector decision:

$$\begin{aligned} \text{IF } Val \geq Tol \quad \text{THEN } & \textit{median filter} \\ \text{ELSE } & \textit{identity filter} \end{aligned} \quad (19)$$

where

$$Val = \sum_{\lambda}^{\lambda+2} |x^* - y_{\lambda}| \quad (20)$$

is a reduced sum of absolute differences between the central sample x^* and the outputs of LUM smoothers y_k for each possible value of tuning parameter k . The output of LUM smoother is given by

$$y_k = \textit{med}\{x_{(k)}, x^*, x_{(N-k+1)}\} \quad (21)$$

where $x_{(k)}$ and $x_{(N-k+1)}$ are lower and upper order statistics of the ordered set. In (19) Tol presents threshold (in the case of gray scale images, the optimal value is 60 for a lower noise corruption or 90 for a high corrupted images [7]) and for image sequences were used values 60 and 90.



Fig. 3 Used image sequence models: (a) Salesman – 5th frame (b) Salesman – 25th frame (c) Susie – 5th frame (d) Susie – 25th frame (e) People – 5th frame (f) People – 25th frame

Note, that in the case of I10 noise $\lambda_{3 \times 3} = 2$, $\lambda_{1,9,1} = 3$ and $\lambda_{9,9,9} = 6$ and threshold $Tol = 60$. For BW20 are considered $\lambda_{3 \times 3} = 3$, $\lambda_{1,9,1} = 4$ and $\lambda_{9,9,9} = 8$ and $Tol = 90$.

4. Experimental results

To achieve the robustness of proposed methods, three dynamic image sequences of various details and the motion complexity (described in [10,11]). Every sequence consists of 30 frames. The used frames had resolution of 256x256 pixels with 8 bits/pixel gray-scale quantization.

These sequence models were corrupted by two types of the impulse noise with uniform distribution of impulses. The first one (Fig. 4a) is the impulse noise with variable random value (in case of 8 bit per pixels quantized image, the original value was replaced by random value between 0 and 255). Mathematically,

$$x(n, i, j) = \begin{cases} z & \text{with probability } p \\ o(n, i, j) & \text{with probability } 1 - p \end{cases} \quad (22)$$

where $x(n, i, j)$ is a corrupted signal, $o(n, i, j)$ describes original signal, n, i, j are indices of sample location and z is random value (impulse) from $\langle 0, 255 \rangle$ with probability p .

The second one type of the impulse noise is the so-called salt and pepper noise (Fig.4b) where pixels of the image were replaced by black and white pixels (values 0 or

255, separately). The noise model of salt and pepper noise is given by

$$x(n, i, j) = \begin{cases} 0 & \text{with probability } p_0 \\ 255 & \text{with probability } p_{255} \\ o(n, i, j) & \text{with probability } 1 - p_0 - p_{255} \end{cases} \quad (23)$$

where 0 denotes a white dot with a probability p_0 and 255 describes a black dot with a probability p_{255} . Others are symbols are related to (22).

To evaluate the degree of damage or the performance of proposed architectures (impulse detector with 3x3 median filter) the following objective criteria such as mean absolute error (MAE), mean square error (MSE) and the cross correlation coefficient ΔR were used. Since the image sequence is 3-D signal [17], in paper mentioned criteria are extended to the 3-D forms. Thus the 3-D MAE and 3-D MSE are given by

$$MAE = \frac{1}{TMN} \sum_{n=1}^T \sum_{i=1}^N \sum_{j=1}^N |o(n, i, j) - x(n, i, j)| \quad (24)$$

$$MSE = \frac{1}{TMN} \sum_{n=1}^T \sum_{i=1}^N \sum_{j=1}^N (o(n, i, j) - x(n, i, j))^2, \quad (25)$$

where o is the original image, x is the filtered (distorted) image, n is the temporal index (frame index), i and j are indices of image sample position. Variable T marks a number of frames, M and N denote the image dimension.

Both criteria well express the detail preservation (by MAE) and the noise suppression (by MSE). However, they do not yield the information about the motion dynamics. On that account was introduced [9] the cross correlation criterion ΔR that evaluates the motion-details preservation.

$$\Delta R = \left| R^o - R^x \right|, \quad (26)$$

where R^o and R^x are the statistical cross-correlations of the original and filtered sequence, respectively. Thus, the cross correlation of signal x is expressed as

$$R = \frac{1}{T} \sum_{n=1}^T \frac{\frac{1}{MN} \left| \sum_{i=1}^M \sum_{j=1}^N (x(n,i,j)x(n,i,j)) - E(n)E(n+1) \right|}{\sigma(n)\sigma(n+1)}, \quad (27)$$

where

$$E(n) = \frac{1}{MN} \sum_{i=1}^M \sum_{j=1}^N x(n,i,j) \quad (28)$$

$$\sigma(n) = \sqrt{\frac{1}{MN} \sum_{i=1}^M \sum_{j=1}^N (x(n,i,j) - E(n,i,j))^2} \quad (29)$$

In previous equations $E(n)$ represents the mean value of the n^{th} frame of the sequence, $\sigma(n)$ is the standard deviation of the n^{th} frame.

The closer to one is the cross correlation coefficient the more static is the sequence [9,10]. It means that particular frames more resemble themselves; therefore the sequence contains less motion. Purpose of the filtration is to achieve the smallest difference of cross correlation coefficients between the original noise-free sequence and the filtered sequence, as defined by (24). Tab. 1 shows the motion complexity of used sequence models. From this table it is seen that sequence People is characterised by the largest motion. Other hand sequence Susie is the simplest model.

Sequence	Salesman	Susie	People
R	0.979	0.983	0.878

Tab. 1 Motion evaluating of original sequences

Since MAE, MSE and ΔR well evaluate the performance of an impulse detector along with a 3x3 median filter, there were needful the criteria for a quantification of lonely impulse detectors. On that account two criteria were introduced [15,16]. Thus, the first one evaluates impulse misclassification (MCL) and second one takes measures of successfully detected impulses (SCL). Mathematically:

$$MCL = \frac{\varepsilon_m}{MNT - \alpha} 100 \quad (30)$$

$$SCL = \frac{\alpha - \varepsilon_c}{\alpha} 100, \quad (31)$$

where ε_m is a number of false detected impulses however noise free samples, ε_c is a number of not detected impulses, α is a number of impulses in the sequence of T frames and a frame dimensions M and N .

In the evaluation 15 pixels around the border were not used. In like manner the first and last three frames were not considered. The pixel bypass around the border was on the ground of border effect [4, 10].

Tables 3-5 show performance of proposed impulse detectors. From these results it can be seen that impulse detectors with temporal windows distinguish by deficient impulse detection. Thus, temporal impulse detectors achieve the high MCL and the low SCL. On that account in the case of temporal detector window the worst results were obtained in term of MAE, MSE and ΔR .

However, in case of spatial and spatiotemporal windows the excellent results were expected. Since many detection methods are based on the principle such as a mean value, a standard deviation, an entropy etc. the well exact estimates are performed from a larger input set. Thus, the spatial or spatiotemporal impulse detectors along with a 3x3 median filter well preserve signal details (include motion details) and remove outliers.

In case of 10% impulse noise with random value (denoted as I10 and shown in Fig. 4a) the best, excellent low MCL criteria was obtained by COSD and LUMsm detectors. Although LUMsm detector (Fig. 4c) does not make best SCL, balance between false and successfully detected impulses resulting to the best noise suppression and the detail preservation in the presence a 3x3 median filter.

If higher noise corruption (Fig. 4d) such as 20% salt & pepper noise (BW20 noise) is investigated the best SCL was obtained by spatiotemporal structures of LCP (Fig. 4f) and LUMsm detectors. In addition, SCL is close to value 100%. Similar to case of I10 noise, robust spatial and spatiotemporal LUMsm, COSD, H, SDV detectors markedly improve results achieved by 3x3 median filter (Tab. 6).

Provided results imply following: Precise impulse detection limits the filter use and thus it reduces blurring that is frequently introduced by inaccurate filter estimate (Fig. 4b, e). Note that principle of COSD and LUMsm detectors exclude possible use of temporal windows of 3 samples. Spatial and spatiotemporal structures were used, only.

Noise	I10			BW20		
Sequence	MAE	MSE	ΔR	MAE	MSE	ΔR
Salesman	7.287	825.1	0.396	23.101	3539.3	0.764
Susie	6.738	688.4	0.337	23.021	3270.8	0.741
People	7.069	772.8	0.352	22.473	3351.7	0.680

Tab. 2 Evaluating of noised sequences

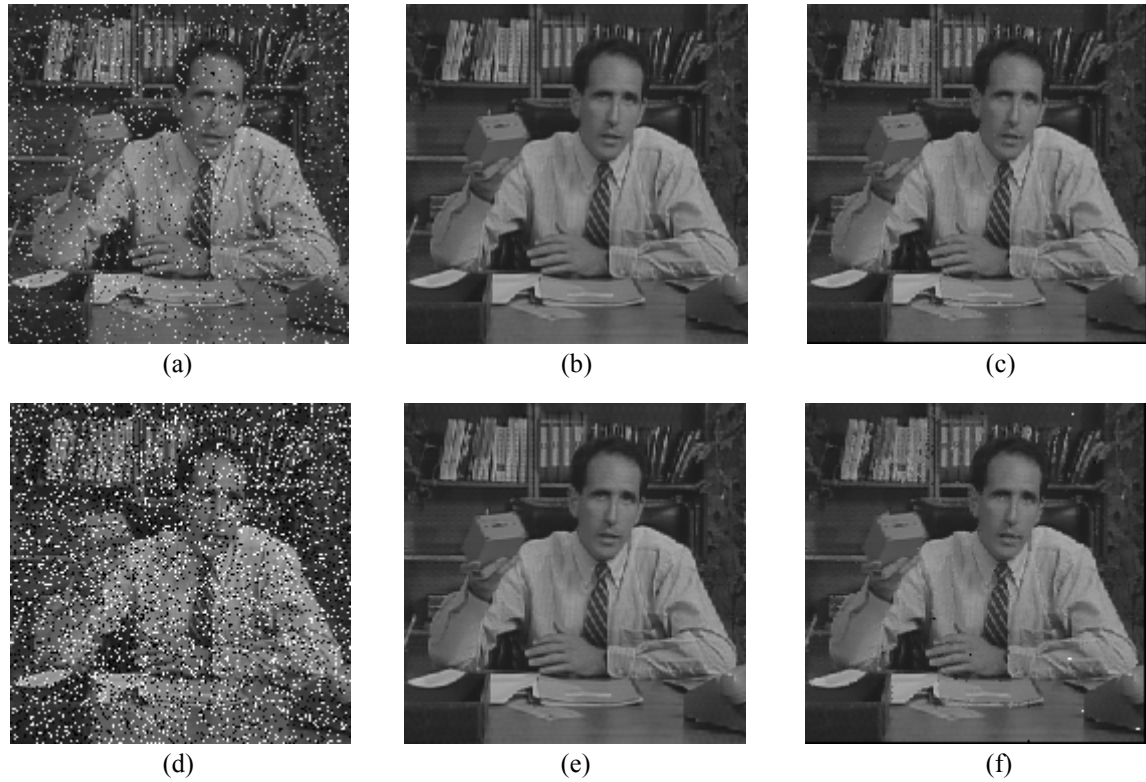


Fig. 4 Salesman - 5th frame (a) Original frame corrupted by I10 noise (b) I10 noise filtered by 3x3 median (c) I10 filtered by ST₁₉₁ LUMsm detector + 3x3 median filter (d) Original frame corrupted by BW20 (e) BW20 filtered by 3x3 median (f) BW20 filtered by ST₉₉₉ LCP detector + 3x3 median filter

Noise		I10					BW20				
Method		Detector		Detector + 3x3 median			Detector		Detector + 3x3 median		
Detector	Window	MCL	SCL	MAE	MSE	ΔR	MCL	SCL	MAE	MSE	ΔR
E	T3	42.291	84.223	2.970	115.5	0.040	37.625	75.471	7.425	761.7	0.247
	3x3 (S)	2.814	62.705	2.174	139.6	0.086	1.183	69.558	5.673	517.9	0.247
	ST _{1,9,1}	1.882	58.067	2.292	159.7	0.098	0.673	65.403	6.167	563.6	0.258
	ST _{9,9,9}	0.177	35.067	3.671	309.4	0.181	0.015	51.655	7.938	728.6	0.287
SDV	T3	47.167	88.777	2.921	92.2	0.029	41.357	79.814	6.833	682.7	0.208
	3x3 (S)	11.717	80.790	2.027	56.2	0.020	4.936	91.147	2.461	99.1	0.053
	ST _{1,9,1}	8.038	80.456	1.553	42.4	0.018	2.735	90.764	2.179	83.4	0.045
	ST _{9,9,9}	3.626	78.240	1.398	38.6	0.013	0.328	90.675	1.960	69.1	0.037
COSD	3x3 (S)	0.460	67.456	1.277	39.8	0.020	2.206	93.000	2.147	84.0	0.044
	ST _{1,9,1}	0.142	67.797	1.124	31.6	0.018	1.437	93.168	1.982	75.8	0.040
	ST _{9,9,9}	0.353	68.667	1.189	34.7	0.016	0.470	94.474	1.775	61.3	0.029
LCP	T3	49.314	90.026	2.944	86.8	0.028	42.979	81.083	6.768	675.6	0.204
	3x3 (S)	17.907	85.543	2.387	56.7	0.015	8.056	99.008	2.181	70.9	0.032
	ST _{1,9,1}	13.845	86.215	1.917	44.3	0.012	5.101	99.360	1.819	57.1	0.027
	ST _{9,9,9}	9.734	86.806	1.844	43.0	0.006	1.661	99.906	1.568	49.5	0.022
H	T3	44.330	88.466	2.874	93.1	0.029	38.941	78.030	7.136	735.4	0.184
	3x3 (S)	11.782	80.090	1.996	55.8	0.021	4.896	88.427	2.745	124.9	0.068
	ST _{1,9,1}	8.198	79.800	1.536	42.1	0.018	2.761	87.466	2.545	113.5	0.062
	ST _{9,9,9}	3.641	77.806	1.388	38.4	0.013	0.304	86.347	2.368	96.2	0.051
LUMsm	3x3 (S)	0.233	74.419	1.005	30.7	0.017	0.143	98.687	1.421	49.4	0.027
	ST _{1,9,1}	0.116	78.183	0.811	18.9	0.009	0.418	96.861	1.703	71.1	0.039
	ST _{9,9,9}	0.087	76.938	0.848	21.4	0.011	0.073	99.445	1.340	43.5	0.023

Tab. 3 Evaluating of filtered sequence Salesman

Noise		I10					BW20				
Method		Detector		Detector + 3x3 median			Detector		Detector + 3x3 median		
Detector	Window	MCL	SCL	MAE	MSE	ΔR	MCL	SCL	MAE	MSE	ΔR
<i>E</i>	<i>T3</i>	22.738	80.728	1.826	83.9	0.028	19.538	75.786	6.303	690.9	0.205
	<i>3x3 (S)</i>	2.620	64.945	1.884	110.8	0.064	1.117	70.010	6.025	595.5	0.249
	<i>ST_{1,9,1}</i>	1.468	59.037	2.094	135.0	0.077	0.511	65.911	6.648	661.5	0.264
	<i>ST_{9,9,9}</i>	0.132	35.177	3.397	261.2	0.146	0.009	50.995	8.889	878.5	0.289
<i>SDV</i>	<i>T3</i>	29.977	86.858	1.821	60.7	0.016	24.993	82.109	5.427	579.2	0.155
	<i>3x3 (S)</i>	11.265	83.608	1.458	29.7	0.008	4.554	96.356	1.554	56.4	0.027
	<i>ST_{1,9,1}</i>	8.536	82.654	1.262	25.7	0.007	2.712	96.874	1.344	43.4	0.020
	<i>ST_{9,9,9}</i>	2.994	80.772	0.927	18.4	0.005	0.139	97.493	1.091	30.0	0.013
<i>COSD</i>	<i>3x3 (S)</i>	0.125	67.732	0.985	25.3	0.012	1.166	97.901	1.217	40.6	0.018
	<i>ST_{1,9,1}</i>	0.080	67.889	0.961	24.0	0.012	1.022	98.071	1.172	38.6	0.017
	<i>ST_{9,9,9}</i>	0.105	68.601	0.943	23.0	0.011	0.133	98.329	1.046	28.7	0.012
<i>LCP</i>	<i>T3</i>	33.905	88.409	1.892	56.2	0.015	27.986	82.930	5.435	574.5	0.152
	<i>3x3 (S)</i>	17.343	88.139	1.708	27.9	0.003	7.150	99.248	1.460	38.0	0.014
	<i>ST_{1,9,1}</i>	14.445	88.265	1.501	23.8	0.003	4.741	99.544	1.276	31.5	0.011
	<i>ST_{9,9,9}</i>	8.776	89.261	1.234	19.2	0.002	0.896	99.801	1.036	25.9	0.010
<i>H</i>	<i>T3</i>	29.890	86.480	1.853	62.7	0.017	24.950	80.770	5.679	610.7	0.143
	<i>3x3 (S)</i>	11.539	82.949	1.462	30.3	0.009	4.678	92.642	2.066	101.8	0.051
	<i>ST_{1,9,1}</i>	8.860	81.848	1.278	26.7	0.008	2.816	92.642	1.911	91.5	0.045
	<i>ST_{9,9,9}</i>	3.140	80.048	0.950	19.2	0.005	0.138	94.330	1.466	58.4	0.028
<i>LUMsm</i>	<i>3x3 (S)</i>	0.048	76.813	0.718	16.3	0.007	0.113	97.789	1.148	43.0	0.021
	<i>ST_{1,9,1}</i>	0.051	80.064	0.618	11.0	0.004	0.058	98.688	1.019	29.9	0.013
	<i>ST_{9,9,9}</i>	0.023	79.631	0.618	11.3	0.004	0.011	98.895	0.981	26.2	0.011

Tab. 4 Evaluating of filtered sequence Susie

Noise		I10					BW20				
Method		Detector		Detector + 3x3 median			Detector		Detector + 3x3 median		
Detector	Window	MCL	SCL	MAE	MSE	ΔR	MCL	SCL	MAE	MSE	ΔR
<i>E</i>	<i>T3</i>	22.245	73.290	2.811	121.3	0.015	19.260	73.719	7.185	747.3	0.177
	<i>3x3 (S)</i>	2.663	62.062	2.297	133.6	0.066	1.175	70.191	5.812	513.4	0.210
	<i>ST_{1,9,1}</i>	1.446	56.204	2.448	156.9	0.079	0.528	65.976	6.278	558.9	0.217
	<i>ST_{9,9,9}</i>	0.204	34.110	3.666	294.0	0.155	0.019	52.120	7.991	719.3	0.234
<i>SDV</i>	<i>T3</i>	33.042	82.346	3.012	93.4	0.008	28.155	79.857	6.744	656.2	0.132
	<i>3x3 (S)</i>	12.669	80.740	2.397	59.0	0.004	5.666	94.088	2.561	92.9	0.025
	<i>ST_{1,9,1}</i>	9.714	79.736	2.113	52.0	0.008	3.537	94.355	2.289	79.6	0.017
	<i>ST_{9,9,9}</i>	5.660	77.715	1.724	43.0	0.011	0.641	96.002	1.777	54.8	0.010
<i>COSD</i>	<i>3x3 (S)</i>	0.322	66.845	1.312	37.9	0.010	1.834	96.855	1.963	67.7	0.018
	<i>ST_{1,9,1}</i>	0.240	67.054	1.264	35.2	0.007	1.548	97.255	1.881	63.5	0.013
	<i>ST_{9,9,9}</i>	0.807	68.073	1.340	37.4	0.002	0.921	98.167	1.707	50.7	0.004
<i>LCP</i>	<i>T3</i>	37.892	84.548	3.166	88.7	0.011	32.433	81.631	6.771	646.4	0.126
	<i>3x3 (S)</i>	20.052	85.563	2.936	62.2	0.015	9.818	99.206	2.581	71.6	0.006
	<i>ST_{1,9,1}</i>	17.479	85.496	2.694	56.5	0.021	7.334	99.532	2.315	62.5	0.005
	<i>ST_{9,9,9}</i>	15.185	85.771	2.452	51.3	0.027	3.370	99.853	1.905	52.1	0.004
<i>H</i>	<i>T3</i>	33.113	81.856	3.024	95.6	0.007	28.134	78.150	7.033	699.4	0.116
	<i>3x3 (S)</i>	12.482	79.996	2.356	58.8	0.003	5.512	90.368	2.956	129.5	0.045
	<i>ST_{1,9,1}</i>	9.540	78.917	2.081	52.0	0.006	3.404	90.122	2.739	118.4	0.037
	<i>ST_{9,9,9}</i>	0.512	77.168	1.713	43.1	0.010	0.570	92.106	2.145	81.3	0.022
<i>LUMsm</i>	<i>3x3 (S)</i>	0.281	73.592	1.128	31.5	0.006	0.426	96.746	1.823	67.8	0.019
	<i>ST_{1,9,1}</i>	0.530	76.793	1.088	27.5	0.003	0.441	97.972	1.694	54.1	0.008
	<i>ST_{9,9,9}</i>	0.538	74.906	1.120	30.2	0.003	0.388	98.147	1.621	48.6	0.005

Tab. 5 Evaluating of filtered sequence People

Noise	I10			BW20		
Sequence	MAE	MSE	ΔR	MAE	MSE	ΔR
Salesman	4.097	64.3	0.003	4.766	106.7	0.032
Susie	3.097	30.9	0.006	3.541	58.7	0.012
People	5.161	76.7	0.038	5.729	113.8	0.014

Tab. 6 Evaluating of 3x3 median filter

5. Conclusion

Proposed structures that include an impulse detector and a median filter for dynamic noised image sequences were proved and successfully tested. Thus, impulse noise is removed and signal-details are preserved, since the filter is applied in the case of impulse detection, only. Obtained results showed that the three dimensional structures of impulse detectors achieved the excellent precision.

Acknowledgement

The work presented in this paper was supported by the Grant Agency of the Ministry of Education and Academy of Science of the Slovak Republic VEGA under Grant No.1/5241/98.

References

- [1] ABREU, E., LIGHSTONE, M., MITRA, S. K., ARAKAWA, K.: A New Efficient Approach for the Removal of Impulse Noise from Highly Corrupted Images. IEEE Transactions on Image Processing, vol. 5, no. 6, June 1996, pp. 1012-1025.
- [2] ARCE, G. R.: Multistage Order Statistic Filters for Image Sequence Processing. IEEE Transactions on Signal Processing, vol. 39, no. 5, May 1991, pp. 1146-1163.
- [3] BEGHDAI, A., KHELLAF, A.: A Noise-Filtering Method Using a Local Information Measure, IEEE Transactions on Image Processing, vol. 6, no. 6, June 1997, pp. 879-882.
- [4] JAROSLAVSKIJ, L. - BAJLA, I.: Metódy a systémy číslicového spracovania obrazov. Alfa - Vydavateľstvo technickej a ekonomickej literatúry, Bratislava, 1989.
- [5] KLEIHORST, R. P., LAGENDIJK, R. L., BIEMOND, J.: Noise Reduction of Image Sequences Using Motion Compensation and Signal Decomposition. IEEE Transactions on Image Processing, vol. 4, no. 3, March 1995, pp. 274-284.
- [6] LUKÁČ, R.: Impulse Detection by Entropy Detector (H - Detector). Journal of Electrical Engineering, vol. 50, no. 9-10, November 1999, pp. 310-312.
- [7] LUKÁČ, R. – MARCHEVSKÝ, S.: Threshold Impulse Detector Based on LUM Smoother (LUMsm Detector), Journal of Electrical Engineering, vol. 51, no. 1-2, 2000, pp. 44-47.
- [8] LUKÁČ, R., MACEKOVÁ, Ľ., MARCHEVSKÝ, S.: Order Statistic Filters in Dynamic Image Sequences Corrupted by Impulse Noise. In: Proceedings of the 4th International Conference DIGITAL SIGNAL PROCESSING '99, Technical University of Košice (Slovakia), 1999, pp. 50-53.
- [9] LUKÁČ, R., STUPÁK, CS., MARCHEVSKÝ, S., MACEKOVÁ, Ľ.: Order-Statistic Filters in Dynamic Image Sequences. Radioengineering, vol. 9, no. 3, September 2000, pp. 8-14.
- [10] LUKÁČ, R, STUPÁK, CS., MARCHEVSKÝ, S.: Neural Networks for Noised Dynamic Image Sequences. Journal of Electrical Engineering, submitted.
- [11] MACEKOVÁ, Ľ., MARCHEVSKÝ, S.: Noisy Dynamic Image Sequences Filtering Based on Order Statistic Filters. In: Proceedings of DSP '97 3rd International Conference on Digital Signal Processing, Herľany (Slovakia), 1997, pp. 274-278.
- [12] MARCHEVSKÝ, S., DRUTAROVSKÝ, M., CHOMAT, O.: Iterative Filtering of Noisy Images by Adaptive Neural Network Filter. In: Proceedings of the Conference New trends in signal processing I, Liptovský Mikuláš, 1996, pp. 118-121.
- [13] STUPÁK, CS.: Digital Image Filtration Based on Local Statistics. 3rd International Scientific Conference Elektro '99, Žilina, May 25-26 1999, pp.106-111.
- [14] STUPÁK, CS.: Neural Impulse Detector. In: Proceedings of International Conference NEW TRENDS IN DIGITAL SIGNAL PROCESSING V, Liptovský Mikuláš (Slovakia), 2000, pp. 323-326.
- [15] STUPÁK, CS., LUKÁČ, R.: Impulse Detection in Grayscale Images. In: Proceedings of the 4th International Conference DIGITAL SIGNAL PROCESSING '99, Technical University of Košice (Slovakia), 1999, pp. 96-99.
- [16] STUPÁK, CS., LUKÁČ, R., MARCHEVSKÝ, S.: Utilization of the Impulse Detectors in the Grayscale Image Filtering. Journal of Electrical Engineering, vol. 51, no. 7-8, 2000, pp. 173-181.
- [17] VIERO, T., NEUVO, Y.: 3-D Median Structures for Image Sequence Filtering and Coding, Tampere University of Technology, Finland.

About authors...

Rastislav LUKÁČ received the Ing. degree at the Technical University of Košice, Slovak Republic, at the Department of Electronics and Multimedial Communications in 1998. Currently, he is Ph.D. student at the Department of Electronics and Multimedial Communications at Technical University of Košice. His research interest includes image filtering, impulse detection, neural network and permutations.